

**NASA Technical Memorandum 81432**

**APPLICATION OF COMPOSITE  
MATERIALS TO TURBOFAN  
ENGINE FAN EXIT GUIDE VANES**

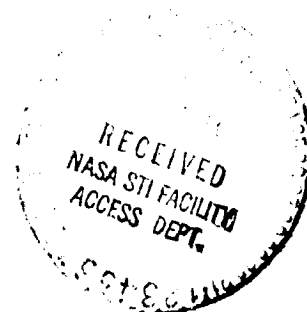
**G. T. Smith  
Lewis Research Center  
Cleveland, Ohio**

**(NASA-TM-81432) APPLICATION OF COMPOSITE  
MATERIALS TO TURBOFAN ENGINE FAN EXIT GUIDE  
VANES (NASA) 19 p HC A02/MF A01 CSCL 11D**

**N80-18106**

**Unclas  
G3/24 47340**

**Prepared for the  
Thirty-fifth Annual Conference of the  
Reinforced Plastics/Composites Institute  
sponsored by the Society of Plastics Industries  
New Orleans, Louisiana, February 4-8, 1980**



# APPLICATION OF COMPOSITE MATERIALS TO TURBOFAN ENGINE

## FAN EXIT GUIDE VANES

G. T. Smith\*

National Aeronautics and Space Administration  
Lewis Research Center  
Cleveland, Ohio

### ABSTRACT

A program was conducted by NASA with the JT9D engine manufacturer to develop a lightweight, cost effective, composite material fan exit guide vane design having satisfactory structural durability for commercial engine use. Based on the results of a previous company supported program, eight graphite/epoxy and graphite-glass/epoxy guide vane designs were evaluated and four were selected for fabrication and testing. Two commercial fabricators each fabricated 13 vanes. Fatigue tests were used to qualify the selected design configurations under nominally dry, 38° C (100° F) and fully wet and 60° C (140° F) environmental conditions. Cost estimates for a production rate of 1000 vanes per month ranged from 1.7 to 2.6 times the cost of an all aluminum vane. This cost is 50 to 80 percent less than the initial program target cost ratio which was 3 times the cost of an aluminum vane. Application to the JT9D commercial engine is projected to provide a weight savings of 236 N (53 lb) per engine.

### INTRODUCTION

The development of implementation technology for more durable, weight efficient, cost effective engine structures is the objective of a recently expanded engine structures research program at the NASA Lewis Research Center. Coordinated programs involving in-house, university and industry activities are being initiated to address difficult engine development problems and to effectively incorporate new analysis techniques and materials developments into currently evolving engine systems. These programs include a substantial effort to exploit the unique mechanical and manufacturing characteristics of newly developed composite material systems. Evaluation of graphite/epoxy composites for fan blades, fan exit guide vanes, engine frames, nacelle components, engine ducts and other relatively low temperature structures are being or have been conducted. The program described in this report is one example.

The fan exit guide vanes (FEGV) of modern high by pass ratio turbofan engines, such as the Pratt and Whitney JT9D, present an opportunity for the application of lightweight graphite/epoxy materials. This structure is aerodynamically loaded and redirects the tangential velocity component of the air flow downstream of the fan blades. No structural loads are carried by the vanes so that a vane failure can cause only minor aerodynamic losses requiring routine corrective maintenance. Substitution of graphite/epoxy vanes for the standard aluminum vanes was expected to provide at least a 50 percent savings in vane weight which could, in turn, provide a significant reduction in direct operating costs to the commercial engine user.

\*Structure and Composites Research Engineer, Structures and Mechanical Technology Division

Pratt and Whitney initiated a program during 1969, intended to develop a graphite fiber reinforced epoxy FEGV capable of sustained operational service. This first relatively limited program resulted in over 700 hours of engine operating experience with a vane designed for the JT9D-3 engine. This engine testing program is described in reference 1. Based on the performance achieved with the JT9D-3 vanes, a large number of vanes were manufactured for the JT9D-70 model engine. Over 4600 hours of engine operating experience including 2630 hours of flight test time were accumulated. During this extensive testing program, airfoil fatigue performance, as well as high material cost and material processing problems were identified. Accordingly, replacement of the composite FEGV in the -70 model engine with conventional all aluminum vanes was desirable.

The program described by this paper was addressed to the partial resolution of the difficulties identified during the JT9D-70 vane test program. Vane design evaluation, vane fabrication, and vane fatigue testing were conducted in order to establish a revised design and qualified manufacturing processes. A complete description of this NASA funded program including all test data, is presented in reference 2.

#### FIRST GENERATION COMPOSITE GUIDE VANE

The relation of the fan exit guide vanes to the overall engine structure is shown in figure 1. As previously noted these vanes do not carry any significant structural load. The front engine frame support is provided by eight large radial struts located immediately downstream of the guide vane position. The number of vanes for a particular engine model are determined by aerodynamic and noise requirements. This number varies from 84 to 108 vanes per engine depending on the particular engine model.

The exit guide vane operational experience, developed over 4600 hours of engine operating time in the JT9-70 engine, revealed a combination of deficiencies which resulted in inadequate structural durability. Figure 2 shows a typical failure encountered during those engine tests. A fatigue failure is centered at the midspan trailing edge of the vane and is clearly the result of excessive first bending mode deflections. Extensive delamination failure of the shell plys on the vane suction surface is present. The pressure surface displays somewhat less damage but the protective polyurethane coating has been peeled off and local chordwise cracking is evident from the midspan trailing edge to about the one third chord location. Figure 3 presents a photomicrograph taken of the vane cross section at midspan. The upper left hand detail shows indications of fiber contamination in the region near the vane trailing edge. Resin rich areas occurring where shell plys are terminated are also evident. The program which was funded by NASA was addressed to upgrading both the vane design and the vane manufacturing processes, and to a fatigue test validation of the revised vanes.

The failure mode experienced during the -70 model engine operations indicated that a reduction in the vane first bending moment deflections coupled with improvements in the physical characteristics of the composite materials were needed to attain adequate operational durability. Changes in both the vane design parameters and in the fiber treatment were made. The design parameter changes included both a change in the external vane contour and a change in the shell lay-up patterns. Figure 4 illustrates the revised trailing edge contour.

The trailing edge thickness was increased and the lay-up pattern modified to provide additional trailing edge stiffness. The modified lay-up pattern is compared with the original -70 model pattern in figure 5. The original thin trailing edge vane was characterized by termination of all shell plys in the trailing edge region. The revised design featured a trailing edge wrap around for the four outer plys resulting in a more continuous ply structure in this critical region of the vane.

#### GUIDE VANE REDESIGN

Eight candidate vane design revisions were screened using NASTRAN finite element analysis. The response to a 34 KPa (5 psi) static pressure load was obtained for each of the eight candidate designs. The calculated results of the radial static strains at the midspan locations, the first bending, and torsion stiffness coefficients, the shear and tension moduli, and the natural frequencies of bending and torsion based on bulk vane modulus properties, are presented in Table I. In addition to the eight candidate vane designs results for the -70 model, all aluminum vane and the -70 model composite vane are included in the table for comparison. The radial static strains are presented for both the midspan maximum thickness location and for the vane midspan trailing edge location which was the apparent failure initiation point in the engine testing program. Candidates 5, 6 and 8 were eliminated due to the high static strain at the vane trailing edge. In addition, the poor compressive strength of the Kevlar core material further detracts from the characteristics of vane number 5 due to compression loading of the trailing edge experienced during flutter excitation of the vanes. Vane number 7 was rejected because of the relatively large static strain at the maximum thickness point and vane 4 was eliminated in preference to a modification of vane 2 containing a glass cloth shell and a 345 GPa (50 msi) modulus graphite core.

As a result of this preliminary vane design analysis, four detail designs were established for additional evaluation. Table II presents the principal characteristics of these vanes. All four designs have a unidirectional, high modulus all-graphite/epoxy core and angle ply shell with a thin 0.254 mm (0.01-in.) thickness aluminum foil leading edge protection system. Two of the designs have graphite shells, two fiberglass shells.

Two vendors were chosen to fabricate the vanes for this program. Composite Horizons Company produced the pultruded core vanes, identified in the upper part of Table II. TRW provided the vanes shown in the lower portion of the table.

All four selected designs contained a high modulus graphite fiber core (Fortafil 5A) to provide adequate bending stiffness. The pultrusion core compression molded vanes were fabricated by Composite Horizons and the ply lay-up, compression molded vanes were fabricated by TRW. Both vendors produced one all-graphite fiber vane design and one graphite core-fiberglass shell design. The Composite Horizons all-graphite vane used the high modulus 331 GPa (48 msi) Fortafil 5A fibers for both the core and shell. The TRW all-graphite vane used the high modulus Fortafil 5A fibers for the core and a lower modulus 331 GPa (32 msi) AS-2 graphite fiber shell. The Composite Horizons glass shell was layed-up with 6581 style S-glass cloth while the TRW glass shell was layed-up with size 449 Owens Corning S-2 glass roving. Both vendors used  $\pm 45$  degrees shell lay-up patterns for the angleply glass shells. The two angleply graphite shell patterns differed very slightly,  $\pm 35$  degrees for Composite Horizons vane and  $\pm 30$  degrees for TRW vane.

The effect of the trailing edge thickness change on the radial strain at the midspan location is shown in figure 6. The radial strain distribution was obtained from a NASTRAN analysis of the high modulus shell - high modulus core, all-graphite design subjected to a 34 KPa (5 psi) static bending load. The radial strain level of the thick trailing edge blade has been significantly reduced, particularly at the trailing edge which was the previous failure initiation location.

The predicted first bending mode stiffness characteristics of the four selected vane designs are compared to the thin trailing edge design in figure 7. The bending spring rate coefficient,  $K_B$ , is indicated for each design. The two all-graphite designs were approximately 35 percent stiffer than the thin trailing edge vane while the S-glass shell designs were about 15 percent stiffer.

The corresponding comparisons of torsional spring rates are shown in figure 8. The revised vane designs with the thick trailing edge show a very much reduced torsional stiffness compared to the thin trailing edge model vane. The all-graphite vanes as before, are somewhat stiffer than the S-glass shell vanes but are still substantially less stiff than the thin trailing edge vane. The effect of these stiffness changes on the 1st bending and on the torsional frequencies can be inferred from figure 9. Here the frequencies of the thin trailing edge vane are compared to the thick vane designs. There appears to be very little change in the first bending mode results; however, the first torsional frequencies have decreased significantly. The least separation between the first torsional excitation frequency and the first bending mode frequency is about 150 Hz for the Fortafil 5A S-glass cloth blade and this difference is believed to provide sufficient margin for prevention of excitation of a coupled bending and torsion vibrational mode.

Both vane fabricators produced a total of 13 vanes for the program. In addition, both provided flat panels for material characterization and certification testing. Samples of neat resins used by each supplier were also tested.

The experience on the -70 model tests indicated improvements in polyurethane coating-to-composite peel strength and in short beam shear strengths were needed. Deficiencies in both of these mechanical characteristics were attributed to the Fortafil 5A fiber surface characteristics. The fiber manufacturer, Great Lakes Carbon Company, undertook development of a surface treatment intended to promote adhesion between the fiber and the epoxy matrix materials. The treatment which was evolved is proprietary. The effect of the relative degree of this treatment on the shear, flexural strength and peel strength is indicated in figure 10. Both the peel strength and shear strength showed significant improvements while the flexural strength was relatively unaffected. The level of surface treatment indicated by the Fortafil 5A specification position on figure 10 was agreed upon by both vane fabricators prior to the initiation of vane fabrication.

#### REDESIGNED GUIDE VANE TESTING

The high frequency fatigue bench testing of the revised vanes was accomplished with a Unholtz-Dickie electrodynamic exciter. The vanes were bonded into cylindrical end fixtures. These end fixtures were clamped to a platen which was subsequently attached to the active element of the Unholtz-Dickie ex-

citer. Prior to mounting the test platen on the fatigue machine, a torque was applied to the cylindrical end fixtures which was sufficient to produce a strain of  $-1750 \mu\epsilon$  on the convex, midspan trailing edge vane in order to simulate the steady state bending moment experienced during engine operation. The tests were conducted by adjusting the exciter frequency until the first bending moment resonance was achieved. A telemicroscope was focused on the midspan trailing edge location and the relationship between the strain gage reading and the displacement indicated by the telemicroscope was established. Generally the strain gage life was limited to a relatively short portion of the test so that the final part of the test was monitored entirely with the telemicroscope.

The entire vane test sequence for the 20 vanes tested is shown in figure 11. After achieving the first bending mode resonance frequency, the exciter amplifier gain was adjusted to produce either a  $1000 \mu\epsilon$  or a  $1200 \mu\epsilon$  dynamic strain amplitude. The vanes were vibrated at this strain amplitude until  $10^7$  cycles had been completed. After completing  $10^7$  strain cycles, the strain amplitude was increased by  $200-400 \mu\epsilon$  and another  $10^7$  cycles accumulated. This sequence was repeated until failure which is indicated on figure 11 by the  $\square$  symbol.

The test results for all four vanes are summarized in figure 12. The data were analyzed by a standard Weibull procedure to establish the minimum strain amplitude for a 1 per 1000 failure rate. This level is indicated in figure 12 for each vane design. Also indicated is the estimated engine operational vibratory strain amplitude based upon measured vane stiffness and the vibratory strain history obtained during the -70 model engine operating experience. The solid data points represent vanes which were moisture conditioned (0.8 percent moisture) and tested at temperature of  $60^\circ \text{C}$  ( $140^\circ \text{F}$ ). The open symbols represent data from nominally dry vanes tested at  $38^\circ \text{C}$  ( $100^\circ \text{F}$ ). Only the maximum strain amplitude surviving  $10^7$  cycles is indicated for each test.

The margin over the engine operational dynamic strain amplitude was greatest for the fiberglass shell vanes. The Composite Horizons vanes exceeded the 1 in 1000 failure run out strain level by 35 percent and the TRW glass shell vanes exceeded that failure strain run out requirement by 46 percent. Both all-graphite vanes also exceeded design requirements. The Composite Horizons all-graphite vanes provided a 27 percent margin and the TRW all-graphite vane a 34 percent margin over the estimated engine operating strain levels.

The failure modes experienced by the all-graphite and the graphite-glass shell vanes were different. Figure 13 indicates schematically the failure patterns developed during the vibratory fatigue tests. Both the all-graphite vanes (20 msi and 18 msi shell modulus) were characterized by midspan transverse cracking at the vane trailing edge. Longitudinal and transverse cracks in the core region were also present in both all-graphite designs at the midspan locations. Based on both visual and radiographic examination of the failed vanes, a failure sequence consisting of a shell-to-core shear failure followed by shell cracking, transverse cracking of the core, and finally, longitudinal core cracking was established as the most probable.

The two fiberglass shell vanes exhibited different failure modes than the all-graphite shell vanes. The highest modulus shell vanes, fabricated by TRW, failed transverse to the span at the vane attachment location. One vane of that group which had the lowest torsional stiffness, failed by a combination of

transverse core cracking at the trailing edge and radial cracking parallel to the trailing edge. Figure 14 presents a photomicrograph of the vane cross section which clearly shows the core cracking and core to shell delamination failures developed during this test. The two small inserts above and below the trailing edge section show the external appearance of the vane at the cross section location. The three stress whitened areas on the convex surface of the vane appear to correspond to the three cracks extending through the core in the photomicrograph.

The other failure mode of the fiberglass shell vanes which involved longitudinal core cracking is illustrated in figure 15. The lower insert shows the very pronounced stress whitened region extending along the span parallel to and about one inch from the trailing edge. In this case core cracking was concentrated in one primary through crack and one secondary part thickness crack. Complete shell cracking is also apparent on the pressure (concave) side of the vane and extensive core-to-shell delamination is evident on the suction side of the vane.

Although the specific failure modes differed among the four vane designs, all vanes exhibited similar fatigue performance capabilities and all designs exceeded the established engine fatigue requirements. The principal design modification responsible for the improved fatigue performance relative to the JT9D-70 model vanes was believed to be the increase in vane trailing edge thickness and the wrap around trailing edge configuration of the outer shell plys.

#### WEIGHT AND COST CHARACTERISTICS OF COMPOSITE FAN EXIT GUIDE VANES

The substitution of composite FEGVs for the JT9D all-aluminum vanes was intended to provide both a direct weight savings and an attendant cost savings arising from the reduced costs of operating lighter engines. The weight of the all-aluminum vane of the same geometry as the composite vane was 533 gms. The weight of the vanes fabricated by Composite Horizons exhibited somewhat less weight scatter than the TRW vanes. The weight variation for the Composite Horizons vanes was 3.5 percent for the all-graphite vanes and 2.5 percent for the glass shell vanes. The corresponding TRW vane weight variations were 7.1 percent and 3.2 percent, respectively. Based on an average weight of 280 gms a weight savings of 236 N (53 lb) per engine can be obtained by use of the all-graphite vanes.

Both vendors were asked to submit a production price estimate for delivery of 1000 vanes per month. An initial target of 3 times the cost of an all-aluminum vane had been established as a pricing goal at the initiation of the program. Only one vendor submitted a bid for 1979 delivery which was 3.3 and 3.0 times the aluminum vane cost for the all-graphite and the graphite-glass vanes respectively. Both vendors made post 1979 delivery costs contingent on upgrading and modernization of production equipment. These projected costs were 2.6 and 2.0 times the cost of the all-aluminum vane for the all-graphite vanes and 2.3 and 1.7 times the cost of the all-aluminum vanes for the graphite-glass vanes. Thus, the graphite core-glass shell vanes, were approximately 7.5 percent less expensive based on the post 1979 cost estimates.

REPRODUCIBILITY OF THE  
ORIGINAL PAGE IS POOR

#### SUMMARY OF RESULTS AND CONCLUSIONS

The principal conclusions and results obtained from the fatigue test evaluation of four modified JT9D engine fan exit guide vanes are as follows:

1. All four revised vane configurations exhibited a fatigue strain capability in excess of the established engine design requirements. The principal design change which resulted in the improved fatigue performance was the increased thickness of the vane trailing edge and the trailing edge wrap around configuration of the outer shell plies.
2. Vanes produced using different processes, different shell fibers, and different epoxy materials showed similar fatigue performance.
3. The presence of up to 0.8 percent moisture did not adversely affect the fatigue performance of the vanes.
4. Utilization of the all-graphite vanes can provide a weight savings of about 236 N (53 lb) per engine compared to use of the current all-aluminum vanes.
5. The glass fiber-shell/graphite-core vanes generally demonstrated better fatigue performance margins than the all-graphite vanes and were approximately seven percent less expensive than the all-graphite vanes.

#### REFERENCES

1. Vitali, V. J., "Graphite Fiber Reinforced Fan Exit Guide Vanes for the JT9D Engine," New Industries Applications for Advanced Materials Technology, SAMPE vol. 19, 1974, pp. 256-261.
2. Blecherman, S. S., "Design, Durability and Low-Cost Processing Technology for Fan Exit Guide Vanes." NASA CR-159677.



TABLE I. - MASTRAN CALCULATED PROPERTIES OF CANDIDATE FAN EXIT GUIDE VANES

CONFIGURATION	$K_0$	$K_T$	$E_{11}$	$G_{12}$	$f_1^I$	$f_1^T$	Radial Static Strain	
	MM/M (lbs/in)	M-W/deg (in-lbs/deg)	CPa (ksi)	CPa (ksi)	$f_1^I$ Hz	$f_1^T$ Hz	Max. Thickness $\epsilon^R$ % Strain	Trailing Edge $\epsilon^R$ % Strain
<b>10.2 cm (4") Chord</b>								
Aluminum	0.219	3.81	73.1	26.2	162	397	0.0887	-0.1528
Thin Trailing Edge	(1251)	(33.7)	(10.6)	(3.8)				
<b>9.1 cm (3.6") Chord</b>								
Original Thin TE Configuration	0.241	3.29	135.1	19.0	220	565	0.1000	-0.2800
345 GPa (50 M) Graphite 0° Core	(1374)	(29.1)	(19.6)	(2.75)				
345 GPa (50 M) Graphite 4-Ply								
+35° Shell								
<b>Candidate Thick TE Configurations</b>								
1. 345 GPa (50 M) Graphite 0° Core	0.339	2.68	142.7	15.5	248	531	0.0847	-0.1720
345 GPa (50 M) Graphite 4-Ply	(1936)	(23.7)	(20.7)	(2.24)				
+35° Shell								
2. 345 GPa (50 M) Graphite 0° Core	0.286	1.38	127.6	7.9	227	393	0.0945	-0.1990
S-Glass 4-Ply +45° Shell	(1634)	(12.2)	(18.5)	(1.15)				
3. 345 GPa (50 M) Graphite 0° Core	0.307	1.91	134.5	11.03	239	465	0.0910	-0.1740
207 GPa (30 M) Graphite 4-Ply	(1750)	(16.9)	(19.5)	(1.60)				
+35° Shell								
4. 207 GPa (30 M) Graphite 0° Core	0.281	2.7	143.4	15.6	230	527	0.1100	-0.2042
345 GPa (50 M) Graphite 7-Ply	(1607)	(23.9)	(20.8)	(2.26)				
+45°, 0°, -45° Shell								
5. Kevlar 0° Core	0.246	2.7	84.8	15.6	230	541	0.1260	-0.2330
345 GPa (50 M) Graphite 7-Ply	(1407)	(23.9)	(12.3)	(2.26)				
+45°, 0°, -45° Shell								
6. Syntactic Foam Core	0.176	2.52	50.5	14.5	177	522	0.2067	-0.2900
345 GPa (50 M) Graphite 7-Ply	(1004)	(22.3)	(7.32)	(2.11)				
+45°, 0°, -45° Shell								
7. Syntactic Foam Core	0.247	2.96	75.2	17.1	216	566	0.1588	-0.2050
345 GPa (50 M) Graphite 11-Ply	(1408)	(26.2)	(10.9)	(2.48)				
+45°, 0°, -45° Shell								
8. 207 GPa (30 M) Graphite Core	0.217	1.71	91.1	9.7	198	424	0.1326	-0.2700
207 GPa (30 M) Graphite 4-Ply	(1238)	(15.1)	(13.2)	(1.40)				
+35° Shell								

<sup>1</sup>Frequency data based on beam theory using bulk vane modulus properties

M = ksi

TABLE II. - SELECTED FAN EXIT GUIDE VANE CONFIGURATIONS AND PROCESSES

Core			Shell	
Fiber Modulus GPa (ksi)	Orien- tation, Degrees	Material	Fiber Modulus GPa (ksi)	Orientation, Degrees
<b>Pultrusion and Compression Molding</b>				
Portafil 5A Graphite	331 (48)	0	Portafil 3A Graphite Plies	331 (48) +35, -35, -35, +35
Portafil 5A Graphite	331 (48)	0	S-Glass Cloth Style 6581	41 (6.0) +45, -45, +45, -45
<b>Ply Lay-up and Compression Molding</b>				
Portafil 5A Graphite	331 (48)	0	AS-2 Graphite Plies	221 (32) +30, -30, +30, -30
Portafil 5A Graphite	331 (48)	0	Owens Corning S-2 Glass Roving 449 Size	83 (12.0) +45, -45, +45, -45

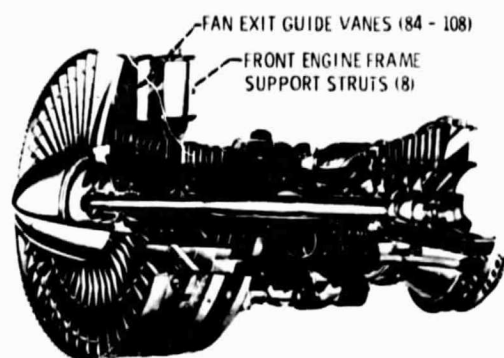


Figure 1. - JT9D turbofan engine.

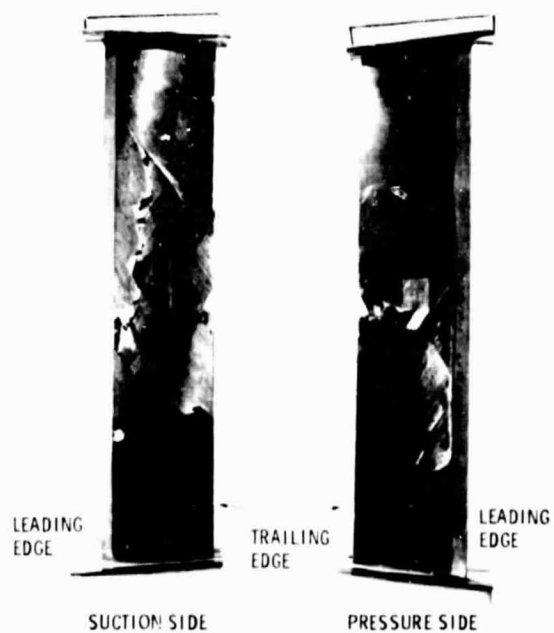


Figure 2. - Vane damage due to engine operation.

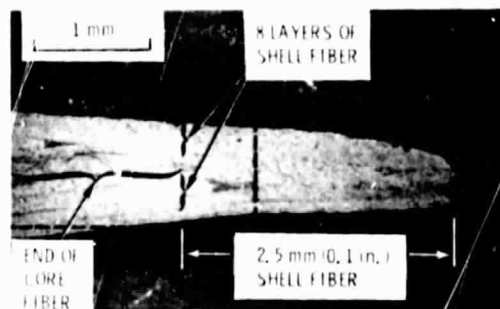
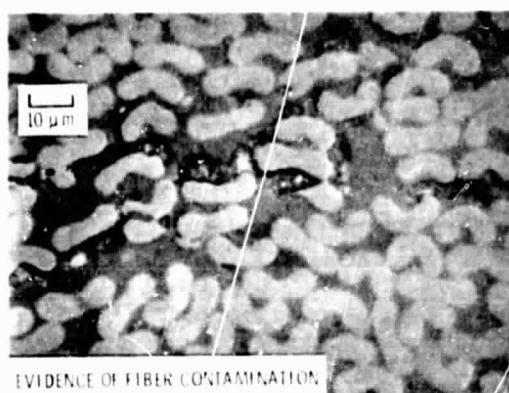


Figure 3. - Fabrication defects in early JT9D fan exit guide vanes.

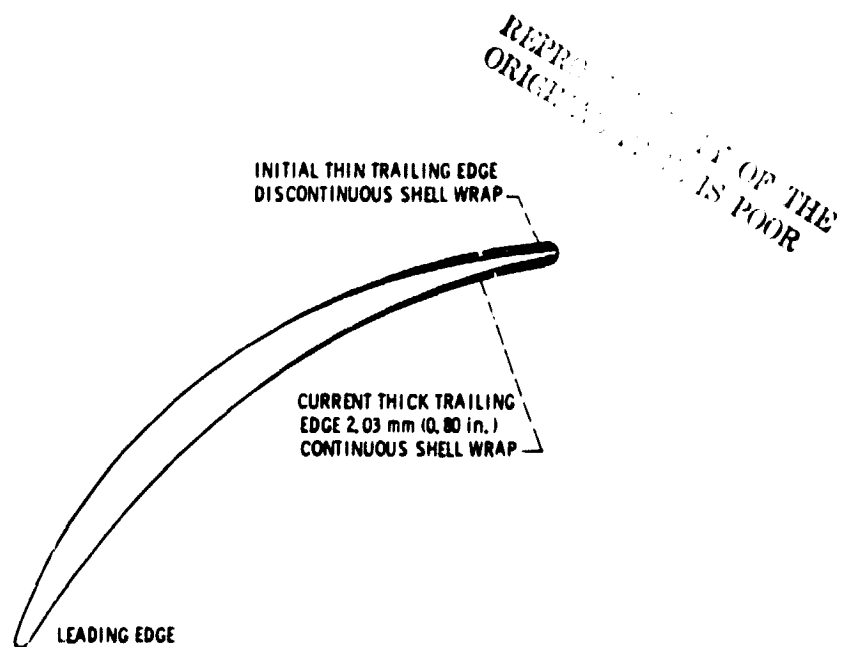


Figure 4. - Initial and current JT9D composite vane cross section.

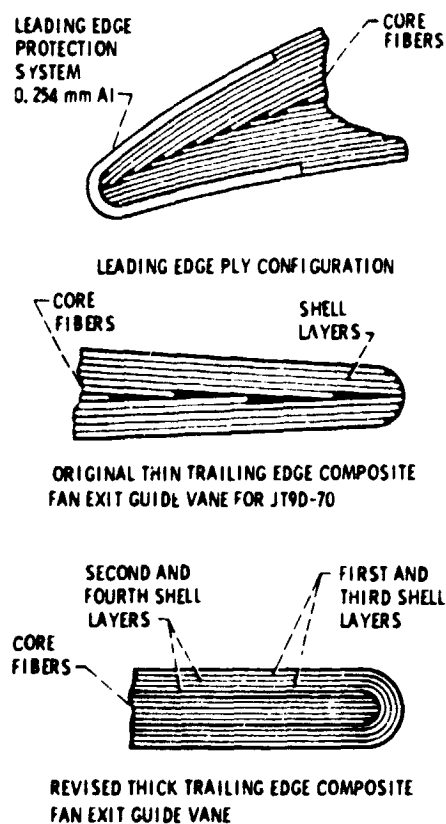


Figure 5. - Comparison of vane ply configurations.

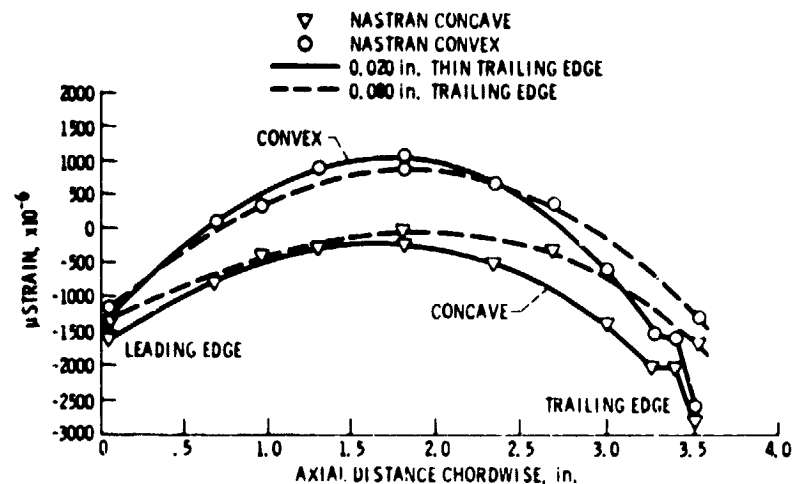


Figure 6. - JT9D composite fan exit guide vane strain distribution-NASTRAN static pressure load analysis 34 KPa (5 psi). Configuration: HMS 50,  $0^\circ$  core; HMS 50  $\pm 35^\circ$  shell.

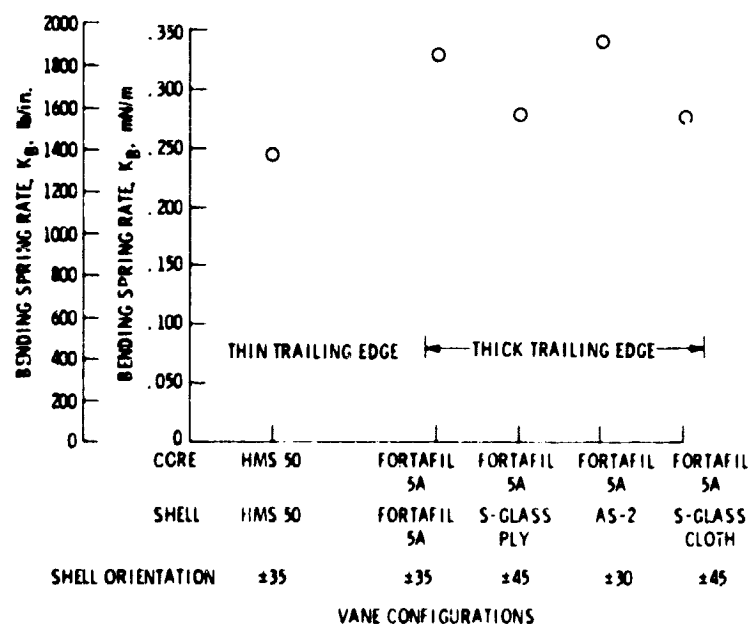


Figure 7. - Composite fan exit guide vane bending stiffness. NASTRAN analysis.

REPRODUCIBILITY OF THE  
ORIGINAL PAGE IS POOR

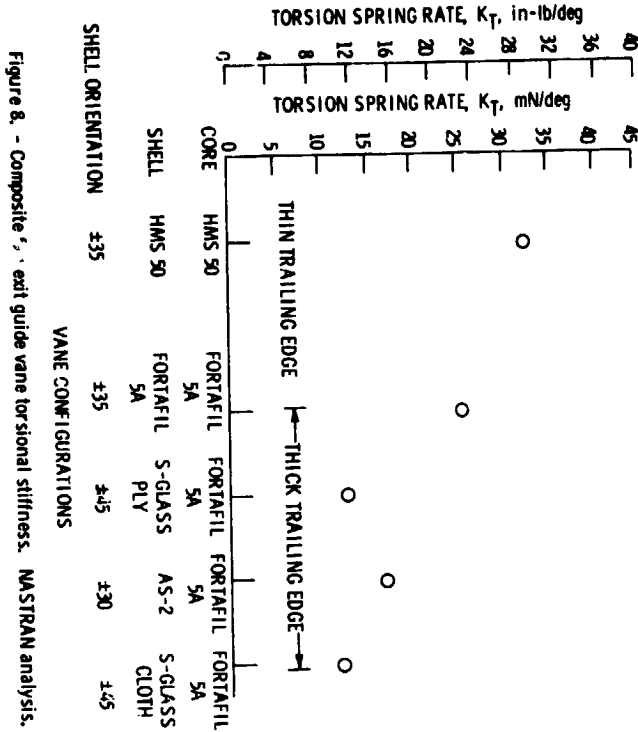


Figure 8. - Composite fan exit guide vane torsional stiffness. NASTRAN analysis.

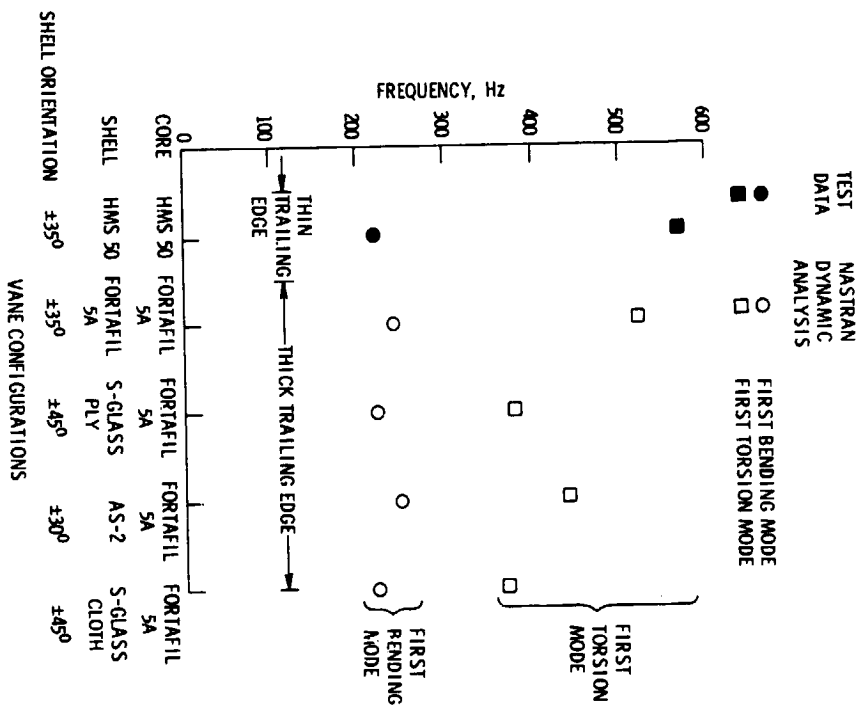


Figure 9. - Composite fan exit guide vane torsion and bending frequency.

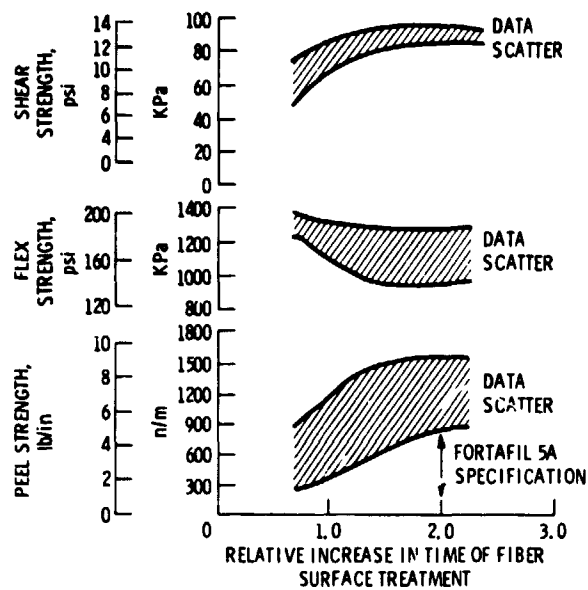


Figure 10. - Composite shear, flexural, and polyurethane peel strength of Fortafil 5A composites vs. relative degree of fiber surface treatment. 60 Volume percent GR/EPON 826 resin specimens data from 1975 period.

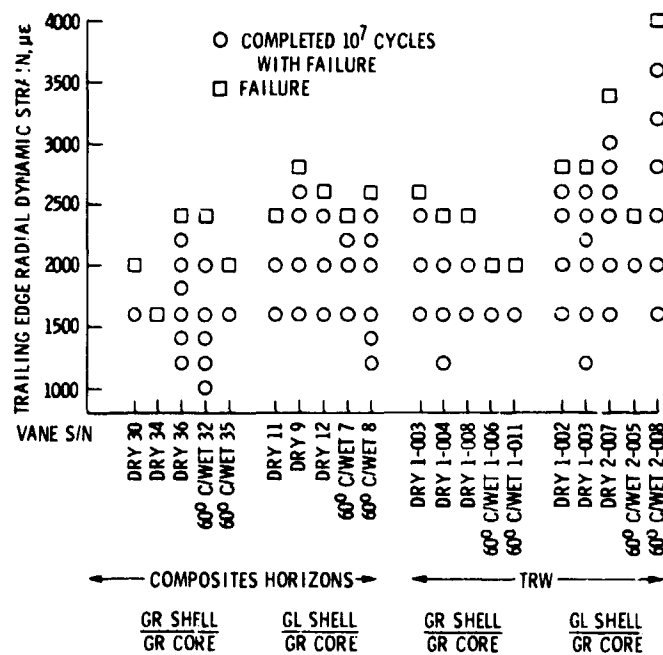


Figure 11. - Composite fan exit guide vane fatigue test sequence.

REPAIRABILITY OF THE  
OLD DESIGN IS POOR

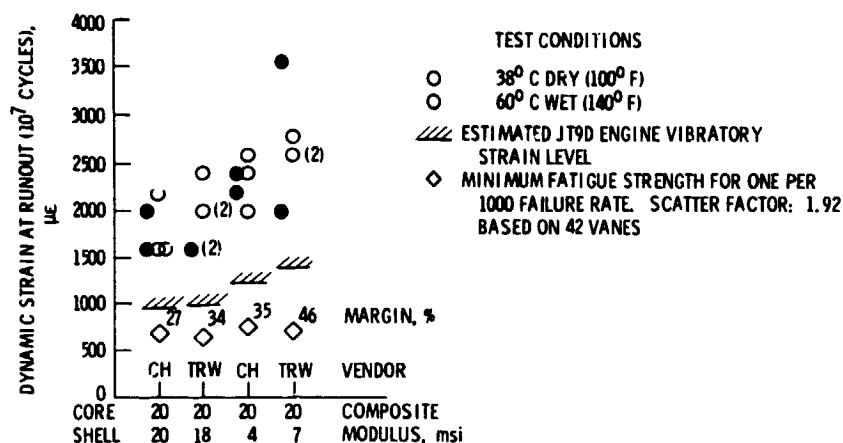


Figure 12. - Comparison of the fatigue performance of revised vane designs.

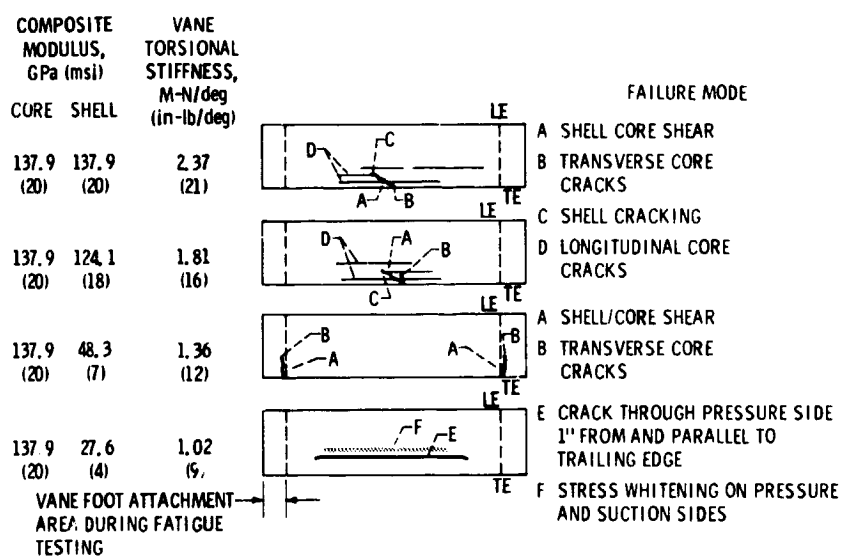


Figure 13. - JT9D composite fan exit guide vane failure modes.



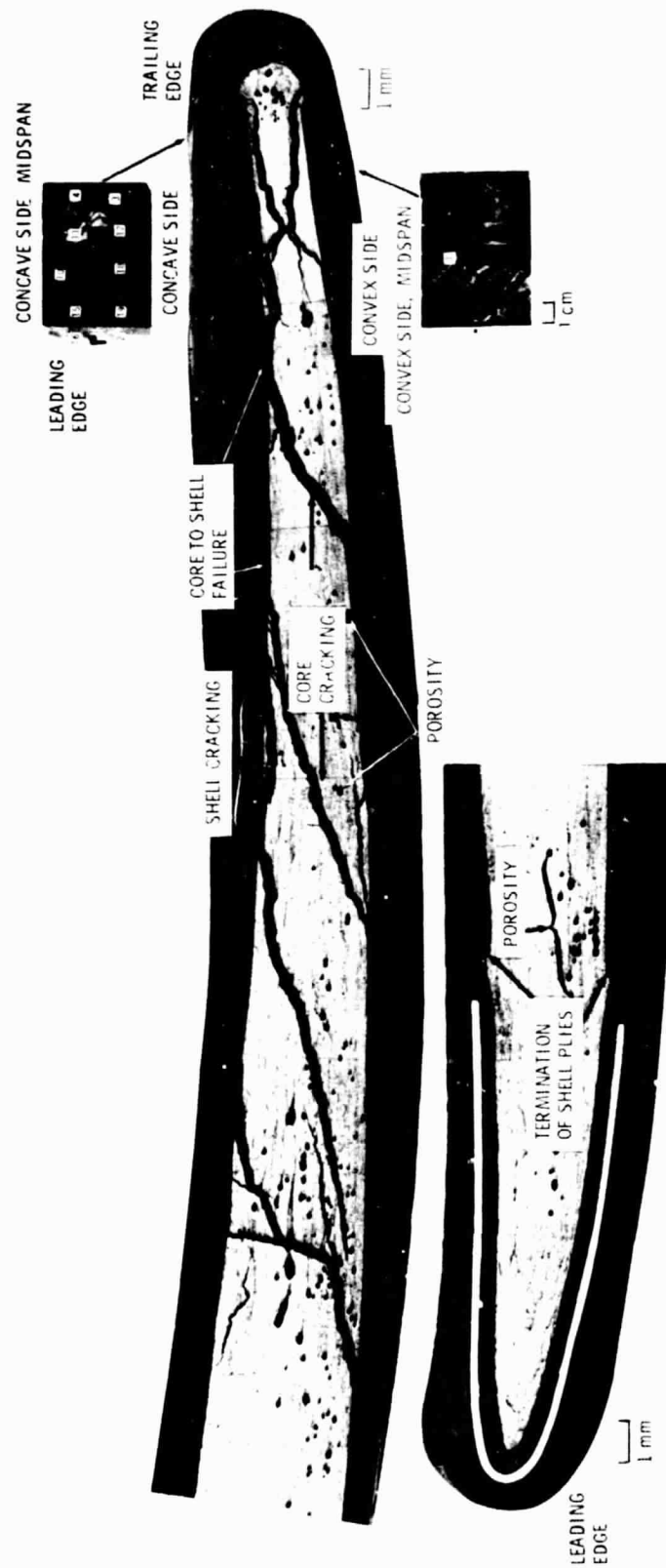


Figure 14. - Photomicrograph of hybrid glass shell-graphite/epoxy core fan exit guide vane fatigue failure.



Figure 15. - Photomicrograph of hybrid glass cloth shell-graphite/epoxy core fan exit guide vane fatigue failure.

REPRODUCTION OF THE  
ORIGINAL IS POOR